ISSN: 0975-833X

Available online at http://www.journalcra.com

International Journal of Current Research
Vol. 12, Issue, 07, pp.12816-12832, July, 2020

DOI: https://doi.org/10.24941/ijcr.38759.07.2020

INTERNATIONAL JOURNAL OF CURRENT RESEARCH

RESEARCH ARTICLE

DIGITAL RESOLUTION OF THE SYSTEM OF GOVERNING EQUATIONS OF THE NATURAL MAGNETOHYDRODYNAMIC CONVECTION PHENOMENON

LANGANFIN GLELE Victor[1], AGBOKPANZO Richard Gilles[2,*] and DEGAN Gérard[1]

[1]Applied Energy and Mechanical Laboratory, Polytechnic school of Abomey-calavi, Benin
[2]Department of Industrial Science and Techniques, Higher Normal School of Technical Education, Benin

ARTICLE INFO

Article History:
Received 07th April, 2020
Received in revised form
25th May, 2020
Accepted 27th June, 2020
Published online 30th July, 2020

Key Words:
Porous Media, Convection, Anisotropy, Magnetic Field.

ABSTRACT

In this study, hydrodynamic and magnetic anisotropies as buoyancy-driven convection effects in a two-dimensional horizontal cavity are investigated analytically. The porous cavity filled with a porous medium is heated isothermally by the sides and its horizontal walls are thermally insulated or conducted gold. The main directions of permeability are oriented in the direction of that is oblique to gravity. Based on scale analysis, solutions for the flow field, temperature distribution, and Nusselt number are obtained. The limiting case corresponding to pure fluid media, and pure porous media, complete these results in order to validate them when compared to those obtained in the literature. It is found that temperature and velocity fields are modified significantlywhen applying the transverse magnetic field. Also, the effects of anisotropic parameters on heat transfer are strongly significant.

Citation: LANGANFIN GLELE Victor, AGBOKPANZO Richard Gilles and DEGAN Gérard1. 2020. "Digital resolution of the system of governing equations of the natural magnetohydrodynamic convection phenomenon", *International Journal of Current Research*, 12, (07), 12816-12832.

INTRODUCTION

The modeling of the magnetohydrodynamic natural convection phenomenon (1, 2, 3, 4), the object of this work, contains differential equations with boundary conditions whose solution can sometimes be obtained analytically(5). However, in most cases, this is not possible and the only possibility is to compute an approximate function using numerical methods (6). The basic idea is to look only for the value of unknown functions at a large number of points: this is termed discretization. Indeed, instead of solving a differential or continuous problem, a large algebraic system called the discrete problem is solved. The discrete problems derived from physical modeling are characterized by their very large size and their resolution could only be envisaged with recent advances in computer science (7, 8). To obtain a discrete problem, numerical methods such as the finite difference method (FDM) (7), the finite element method (FEM)(9, 10), and the finite volumes method (FVM), which are the basis of many software (7), are used. In this work, we adopted two of the three methods mentioned above namely the finite difference method and the finite element method, since they are quick to design, robust and flexible with the existence of a weak solution. The main goal of this article is to present the method of numerical resolution of the phenomenon of natural magneto hydrodynamic convection in a porous cavity.

H'	height of the cavity
L'	width of the cavity
A	aspect ratio of the cavity,
a,b, c, d, e	constants of governing equations
f, g, h, l, m,	constants of governing discrete equations p, q, s
C_p	specific heat at constant pressure
Da	Darcy number

Corresponding author: **AGBOKPANZO Richard Gilles**
Department of Industrial Science and Techniques, Higher Normal School of Technical Education, Benin

g	gravitational acceleration
Ha	Hartmann number
$i\max+2$	number of sub-areas in the horizontal direction
$j\max+2$	number of sub-areas in the vertical direction
k	thermal conductivity
K	permeability tensor
K_1, K_2	permeabilities along the principal axes
K^*	ratio of the permeability
Nu	Nusselt number
Ra	Rayleigh number
T	temperature dimensionless
T'_1	dimensional temperature to the cold wall
T'_2	dimensional temperature in the hot wall
$\Delta T'$	dimensional wall temperature difference $(T'_2 - T'_1)$
Ox ', Oy'	Cartesian coordinate axes
p'	pressure
dx	dimension of a sub-field in the horizontal direction
dy	dimension of a sub-field in the vertical direction
t	time
x'_r, y'_r	Cartesian coordinates corresponding to the principal axes
x, y	dimensional Cartesian coordinates
u'_r, v'_r	relative speeds in the directions x'_r and y'_r respectively
u, v	dimensionless velocities in the directions Ox and Oy
U	dimensionless horizontal velocity
V	vertical speed dimensionless

Greek letters

α	thermal diffusivity
σ	ratio of heat capacities
β	coefficient of thermal expansion of the fluid
λ	relative viscosity
γ	electrical conductivity of the fluid
θ	orientation angle of the main directions of permeability tensor
φ	General dependent value
μ	dynamic viscosity of the fluid
μ_{eff}	apparent dynamic viscosity for the Brinkman model
ρ	density of the fluid
ν	kinematic viscosity of the fluid
	the porous medium porosity
$(\rho_r C_p)_m$	heat capacity of the porous medium
$(\rho_r C_p)_f$	heat capacity of the fluid
ψ	stream function dimensionless

vectors

g	gravitational acceleration
B	transverse magnetic field
J'_r	density of the main current
J'	current density

mathematical operators

∇	vector Nabla
∂	partial derivative

Indices and superscript

i	index of a given mesh point x
j	index of a given mesh point y
n	on the nth iteration
$n+1$	on the nth + 1 iteration

'	on dimensional variables
Others	
$\{\ \}$	vector representation
$[\ ]$	matrix representation

MATERIALS AND METHODS

The numerical resolution of the natural convection phenomena is used in many works**(11, 12)** as it is the case in this study.

Numerical discretization methods: The numerical methods of discretization mentioned previously consist in reducing the resolution of the system of differential equations in the field of study, with appropriate boundary conditions, to those of a system of algebraic equations whose solution gives the desired unknowns (6).

Method of Finite Differences (MFD)

The finite difference method presents a technique for solving partial differential equations, by approximating derivatives by finite differences. This method consists in subdividing the domain of study into a determined number of nodes and in representing the function desired in each of the nodes of the domain by a development limited in Taylor series. Thus, the differential equation is transformed into an algebraic equation for each node. The resolution of the system of algebraic equations makes it possible to obtain the distribution of the function studied in the field of study. This method consists in replacing the partial derivatives by divided differences or combinations of point values of the function, in a finite number of discrete points or nodes of the mesh.

Consider the following regular 1D mesh:

with:

$$dx = x_i - x_{i-1} = x_{i+1} - x_i$$

We express the partial derivatives, we have the partial derivatives are expressed as a function of the values at the discretization points, thus giving:

$$\left[\frac{\partial^2 \varphi}{\partial^2 x}\right]_i = \frac{\varphi_{i+1} - 2\varphi_i + \varphi_{i-1}}{\Delta x^2} \tag{1}$$

And

$$\left[\frac{\partial \varphi}{\partial x}\right]_i = \begin{cases} \dfrac{\varphi_{i+1} - \varphi_i}{\Delta x} & \text{Off-to-the right diagram} \\ \dfrac{\varphi_i - \varphi_{i-1}}{\Delta x} & \text{Off-to-the left diagram} \\ \dfrac{\varphi_{i+1} - \varphi_{i-1}}{2\Delta x} & \text{Centered diagram} \end{cases} \tag{2}$$

It may be noted that a priori, there is a choice between the three forms of approximation of the first derivative. The off-center to the right diagram is the one that has been chosen to approximate the partial derivatives of order one in this work

Finite Element Method (FEM): This method consists in transforming the differential equations into integral forms based on the concept of minimization of a quantity (like heat ...), leading to the exact solution. In other words, it is aimed at finding a global function representing the mathematical model in the field studied. The fundamental principle of the finite element method consists in**(9, 10)**:

- Defining a partition of the study area, that is to say, subdividing the study area into elementary regions (Finite Elements);
- Representing the unknown function on each of these elements by a polynomial approximation;
- Building the integral forms;
- Minimizing the integral forms;
- Organizing calculations in matrix form;
- Solving the algebraic system obtained.

FEM is a very powerful method for solving partial differential equations, especially in complex geometries. Its implementation, on the other hand, is quite complicated and requires a relatively large memory space.

Discretization of the terms of the governing equations

Discretization of the momentum equation

$$\left(K^* \sin^2\theta + \cos^2\theta\right)\frac{\partial^2\psi}{\partial x^2} + \left(\left(1-K^*\right)\sin 2\theta\right)\frac{\partial^2\psi}{\partial x\partial y} + \left(K^*\cos^2\theta + \sin^2\theta + \frac{K_2\beta^2\gamma}{\nu\rho r}\right)\frac{\partial^2\psi}{\partial y^2}$$
$$= -\frac{K_2 g\beta}{\nu}\frac{\partial T}{\partial x} + \frac{K_2\mu_{eff}}{\nu\rho r}\left(\frac{\partial^4\psi}{\partial x^4} + 2\frac{\partial^4\psi}{\partial x^2\partial y^2} + \frac{\partial^4\psi}{\partial y^4}\right) \quad (3)$$

In dimensionless form, it becomes:

$$a\frac{\partial^2\psi}{\partial x^2} + b\frac{\partial^2\psi}{\partial x\partial y} + c\frac{\partial^2\psi}{\partial y^2} = d\frac{\partial T}{\partial x} + e\left(\frac{\partial^4\psi}{\partial x^4} + 2\frac{\partial^4\psi}{\partial x^2\partial y^2} + \frac{\partial^4\psi}{\partial y^4}\right) \quad (4)$$

The distribution of all the terms of the equation gives:

$$a\left[\frac{\partial^2\psi}{\partial x^2}\right]_{i,j} + b\left[\frac{\partial^2\psi}{\partial x\partial y}\right]_{i,j} + c\left[\frac{\partial^2\psi}{\partial y^2}\right]_{i,j} = d\left[\frac{\partial T}{\partial x}\right]_{i,j} + e\left[\frac{\partial^4\psi}{\partial x^4}\right]_{i,j} + 2e\left[\frac{\partial^4\psi}{\partial x^2}\right]_{i,j} + e\left[\frac{\partial^4\psi}{\partial y^4}\right]_{i,j} \quad (5)$$

To discretize these different terms, we started from the Taylor expansion with two variables to obtain a linear system, easily solved by the matrix method:

$$f(x_i + l, y_j + m) = f(x_i + ldx, y_j + mdy) = \sum_{0\le k\le n}\left[\frac{1}{(n-k)!k!}\left(\frac{\partial}{\partial x}\right)^{n-k}\left(\frac{\partial}{\partial y}\right)^{k} f\left(x_i, y_j\right)(ldx)^{n-k}(mdy)^k\right]$$

This formula allows to define the lines of the discretization matrix from the following vector:

VL = (t * Dx, m * Dy, (L * Dx) ^ 2/2, m * W * Dx * Dy, (m * Dy) ^ 2/2, (L * Dx) ^ 3/6, (1 * Dx) * 2 ^ (m * Dy) / 2, (1 * Dx) * (m * Dy) ^ 2/2, (M * Dy) ^ 3/6, (L * Dx) ^ 4/24, (L * Dx) ^ 3 * (m * Dy) / 6 (L * Dx) ^ 2 * (m * Dy) ^ 2/4, (1 * Dx) * (m * Dy) ^ 3/6, (m * Dy) ^ 4/24, (1 * Dx) ^ 5/120 (1 * Dx) ^ 4 * (m * Dy) / 24 (1 * Dx) ^ 3 * (m * Dy) ^ 2/12, (1 * Dx) ^ 2 * (m * Dy) ^ 3/12, (1 * Dx) * (m Dy *) ^ 4/24, (m * Dy) ^ 5/120)

For example, for l = 0 and m = 1, fi, j + 1 and the corresponding line in the discretization matrix is:

VL = (0, Dy, 0, 0, Dy ^ 2/2, 0, 0, 0, Dy ^ 3/6, 0, 0, 0, 0, Dy ^ 4/24, 0, 0, 0, 0 , 0, Dy ^ 5/120)

The procedure is the same for the other values of l and m.

Thus, the discretized terms are obtained from the system resolution:

$$M = \left[\frac{(l*dx)^{n-k}(m*dy)^k}{(n-k)!k!}\right] \text{ with } 0 \le k \le n$$
$$B = \left\{f_{i+l,j+m} - f_{i,j}\right\}$$
$$\left\{\frac{\partial^n f}{\partial x^{n-k}\partial^k}\right\} = inv(M) * B \text{ with } 0 \le k \le n$$

From this resolution, the expressions of each discretized term of the system of governing equations established in this study are obtained as follows:

$$\left[\frac{\partial^2\psi}{\partial x^2}\right]_{i,j} = \frac{\psi_{i+1,j} - 2\psi_{i,j} + \psi_{i-1,j}}{\Delta x^2} \tag{6}$$

$$\left[\frac{\partial^2\psi}{\partial x\partial y}\right]_{i,j} = \frac{\psi_{i+1,j+1} - \psi_{i+1,j-1} + \psi_{i-1,j-1} - \psi_{i-1,j+1}}{4\Delta x\Delta y} \tag{7}$$

$$\left[\frac{\partial^2\psi}{\partial y^2}\right]_{i,j} = \frac{\psi_{i,j+1} - 2\psi_{i,j} + \psi_{i,j-1}}{\Delta y^2} \tag{8}$$

$$\left[\frac{\partial T}{\partial x}\right]_{i,j} = \frac{T_{i+1,j} - T_{i,j}}{\Delta x} \tag{9}$$

$$\left[\frac{\partial^4\psi}{\partial x^4}\right]_{i,j} = \frac{\psi_{i+2,j} - 4\psi_{i+1,j} + 6\psi_{i,j} - 4\psi_{i-1,j} + \psi_{i-2,j}}{\Delta x^4} \tag{10}$$

$$\left[\frac{\partial^4\psi}{\partial x^2\partial y^2}\right] = \frac{\psi_{i-1,j+1} - 2\psi_{i,j+1} + \psi_{i+1,j+1} - 2\psi_{i-1,j} + 4\psi_{i,j} - 2\psi_{i+1,j} + \psi_{i-1,j-1} - 2\psi_{i,j-1} + \psi_{i+1,j-1}}{4\Delta x^2\Delta y^2} \tag{11}$$

$$\left[\frac{\partial^4\psi}{\partial y^4}\right]_{i,j} = \frac{\psi_{i,j+2} - 4\psi_{i,j+1} + 6\psi_{i,j} - 4\psi_{i,j-1} + \psi_{i,j-2}}{\Delta y^4} \tag{12}$$

Grouping of all discretized terms

After regrouping all the discretized terms and their arrangement, the first linear equation of the system is obtained:

$$\begin{aligned} &-q\psi_{i-2,j} + f\psi_{i-1,j-1} + h\psi_{i-1,j} - g\psi_{i-1,j+1} - p\psi_{i,j-2} + l\psi_{i,j-1} - m\psi_{i,j} + l\psi_{i,j+1} \\ &-p\psi_{i,j+2} - g\psi_{i+1,j-1} + h\psi_{i+1,j} + f\psi_{i+1,j+1} - q\psi_{i+2,j} = s(T_{i+1,j} - T_{i,j}) \end{aligned} \tag{13}$$

Where coefficients *f, h, l, m, g, s, p*, and *q* are defined by:

$$g = \frac{b*\Delta x^3*\Delta y^3}{4} + \frac{e*\Delta x^2*\Delta y^2}{2} \tag{14}$$

$$f = \frac{b*\Delta x^3*\Delta y^3}{4} - \frac{e*\Delta x^2*\Delta y^2}{2} \tag{15}$$

$$h = a*\Delta x^2*\Delta y^4 + 4*e*\Delta y^4 + e*\Delta x^2*\Delta y^2 \tag{16}$$

$$l = c*\Delta x^4*\Delta y^2 + 4*e*\Delta x^4 + e*\Delta x^2*\Delta y^2 \tag{17}$$

$$p = e*\Delta x^4 \tag{18}$$

$$q = e*\Delta y^4 \tag{19}$$

$$s = d*\Delta x^3*\Delta y^4 \tag{20}$$

$$m = (2*a*\Delta x^2*\Delta y^4) + 2*a*\Delta x^4*\Delta y^2 + 6*e*(\Delta x^4 + \Delta y^4) + 2*\Delta x^2*\Delta y^2 \tag{21}$$

Discretization of the energy equation

$$\sigma\frac{\partial T}{\partial t}+u\frac{\partial T}{\partial x}+v\frac{\partial T}{\partial y}=\alpha\frac{\partial^2 T}{\partial x^2}+\alpha\frac{\partial^2 T}{\partial y^2},\alpha=1,\sigma=1 \tag{22}$$

$$\sigma\frac{\partial T}{\partial t}+u\frac{\partial T}{\partial x}+v\frac{\partial T}{\partial y}=\alpha\frac{\partial^2 T}{\partial x^2}+\alpha\frac{\partial^2 T}{\partial y^2},\alpha=1,\sigma=1 \tag{23}$$

$$\left[\frac{\partial T}{\partial t}\right]_{i,j}^{n+1}+U_{i,j}\left[\frac{\partial T}{\partial x}\right]_{i,j}+V_{i,j}\left[\frac{\partial T}{\partial x}\right]_{i,j}=\left[\frac{\partial^2 T}{\partial x^2}\right]_{i,j}+\left[\frac{\partial^2 T}{\partial y^2}\right]_{i,j} \tag{24}$$

is given by the method used in the preceding section by:

$$\left[\frac{\partial T}{\partial t}\right]_{i,j}^{n+1}=\frac{T_{i,j}^{n+1}-T_{i,j}^{n}}{dt}=0$$

Because the upper and lower walls of the cavity are adiabatic and there is no energy exchange with the external environment.

$$\left[\frac{\partial T}{\partial x}\right]_{i,j}=\frac{T_{i+1,j}-T_{i,j}}{\Delta x} \tag{25}$$

$$\left[\frac{\partial T}{\partial y}\right]_{i,j}=\frac{T_{i,j+1}-T_{i,j}}{\Delta y} \tag{26}$$

$$\left[\frac{\partial^2 T}{\partial x^2}\right]_{i,j}=\frac{T_{i+1,j}-2T_{i,j}+T_{i-1,j}}{\Delta x^2} \tag{27}$$

$$\left[\frac{\partial^2 T}{\partial y^2}\right]_{i,j}=\frac{T_{i,j+1}-2T_{i,j}+T_{i,j-1}}{\Delta y^2} \tag{28}$$

After discretization and arrangement of all the terms, a second linear equation is obtained:

$$T_{i,j}=\frac{\left(\Delta y^2-\Delta x\Delta y^2\times U_{i,j}\right)\times T_{i+1,j}+\left(\Delta x^2-\Delta x\Delta y^2\times V_{i,j}\right)\times T_{i,j+1}+\Delta y^2\times T_{i-1,j}+\Delta x^2\times T_{i,j-1}}{\left(2\Delta x^2+2\Delta y^2-\Delta x\Delta y^2\times U_{i,j}-\Delta x^2\Delta y\times V_{i,j}\right)} \tag{29}$$

This equation describes the distribution of the temperature function within the cavity which is a function of the flow velocities in both directions.

Discretization of continuity equations: In the same manner, as above, the discretization of the continuity equation is given by:

$$\begin{cases}U_{i,j}=\dfrac{\psi_{i,j+1}-\psi_{i,j}}{\Delta y}\\ V_{i,j}=\dfrac{\psi_{i,j}-\psi_{i+1,j}}{\Delta x}\end{cases} \tag{30}$$

System of discretized governing equations: By putting together the three discretized equations, we obtain the following discretized equation system is obtained:

$$\begin{cases} U_{i,j} = \dfrac{\psi_{i,j+1} - \psi_{i,j}}{\Delta y} \\ V_{i,j} = \dfrac{\psi_{i,j} - \psi_{i+1,j}}{\Delta x} \\ -q\psi_{i-2,j} + f\psi_{i-1,j-1} + h\psi_{i-1,j} - g\psi_{i-1,j+1} - p\psi_{i,j-2} + l\psi_{i,j-1} - m\psi_{i,j} + l\psi_{i,j+1} - p\psi_{i,j+2} - g\psi_{i+1,j-1} \\ + h\psi_{i+1,j} + f\psi_{i+1,j+1} - q\psi_{i+2,j} = s\left(T_{i+1,j} - T_{i,j}\right) \\ T_{i,j} = \dfrac{\left(\Delta y^2 - \Delta x\Delta y^2 \times U_{i,j}\right) \times T_{i+1,j} + \left(\Delta x^2 - \Delta x\Delta y^2 \times V_{i,j}\right) \times T_{i,j+1} + \Delta x\Delta y^2 \times T_{i-1,j} + \Delta x^2 \times T_{i,j-1}}{\left(2\Delta x^2 + 2\Delta y^2 - \Delta x\Delta y^2 \times U_{i,j} - \Delta x^2\Delta y \times V_{i,j}\right)} \end{cases} \quad (31)$$

Discretization of the heat transfer rate: The discretization of the equation of heat transfer rate gives:

$$Nu = \frac{1}{A}\left(\frac{T_{i,j+1} - T_{i,j}}{\Delta x} - U_{i,j}T_{i,j}\right) \quad (32)$$

Schematic resolution of the discretized equations

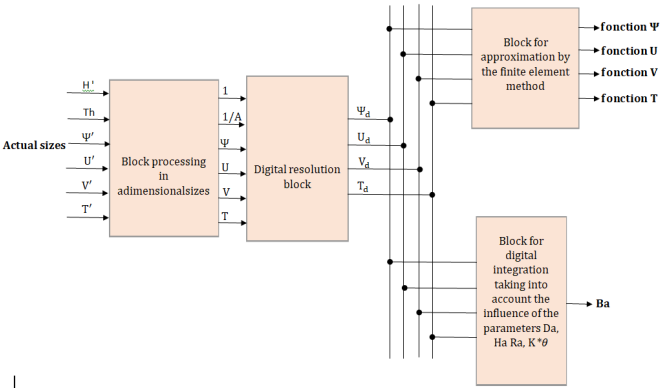

Figure 0-1: Digital resolution diagram

Once the discrete values of the current functions, speeds and temperature are known, the method of the finite elements **(9, 10)** is used to approximate the said functions by continuous functions in an X and Y plane. For the approximation by the finite element method, a reference frame made up of 9 points has been considered.

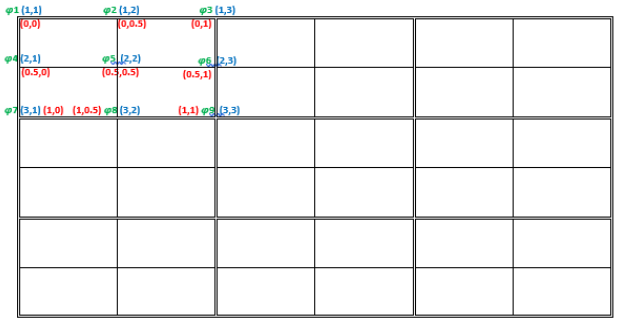

NB: this diagram gives the nodal values of the function corresponding to the current, to the components of the speed or to the temperature Polynomial basis:

The coordinates of the reference points are (0,0); (0, 0.5); (0, 1); (0.5, 0); (0.5, 0.5); (0.5, 1); (1, 0); (1, 0.5); (1, 1). At each of these reference points are associated nodal values made of the values obtained by the discretization of the current, speed U, and V speed features and temperature designated respectively as Si, Ui, Vi, and Ti. The polynomial basis associated with the 9 points is:

(1, m, n, m * m, m * n, n * n, m * m * n * n * m n, m * m * n * n)

Materials: The numerical resolution of the system of discretized governing equations obtained above was performed using the Matlab software (7).

RESULTS AND DISCUSSION

In this section, we present the numerical results obtained in the case of natural magnetohydrodynamic convection in a porous cavity.

Influence of the Hartmann number (Ha) on the speeds U and V: The speed of the convection phenomenon is expressed along the vertical and horizontal axes of the porous cavity. In the present study, the speed relative to the horizontal axis is called *U* and that relative to the vertical axis is designated *V*.

Case Ha = 1

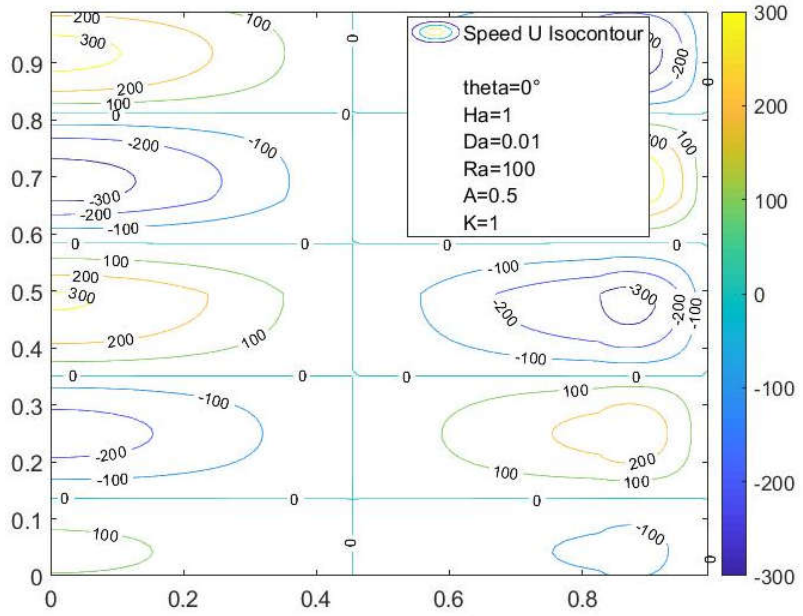

Figure 0-1: Speed U, Case Ha = 1

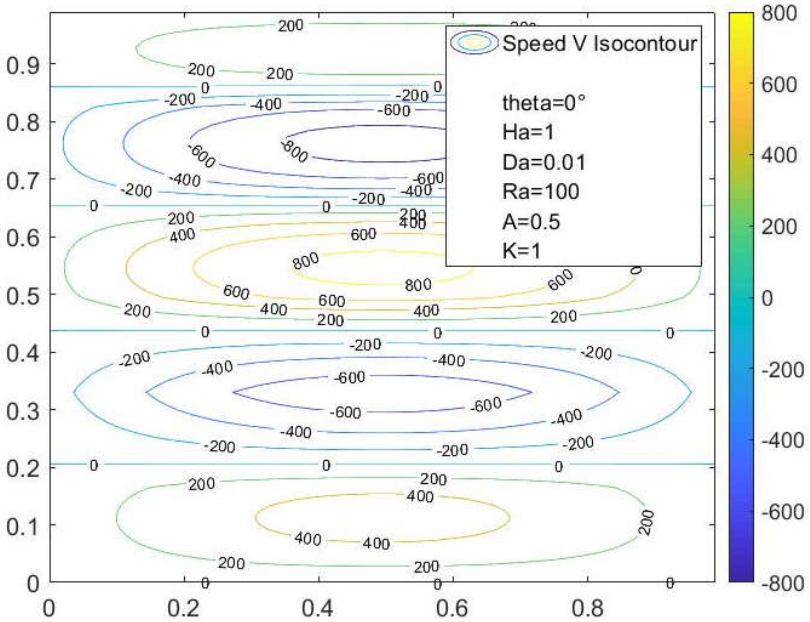

Figure 0-2: Speed V, Case Ha = 1

Case Ha = 2

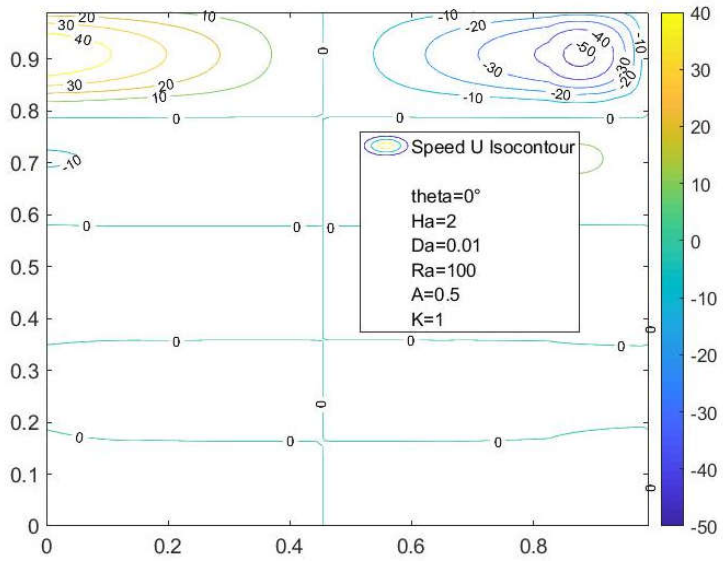

Figure 0-3: Speed U, Case Ha = 2

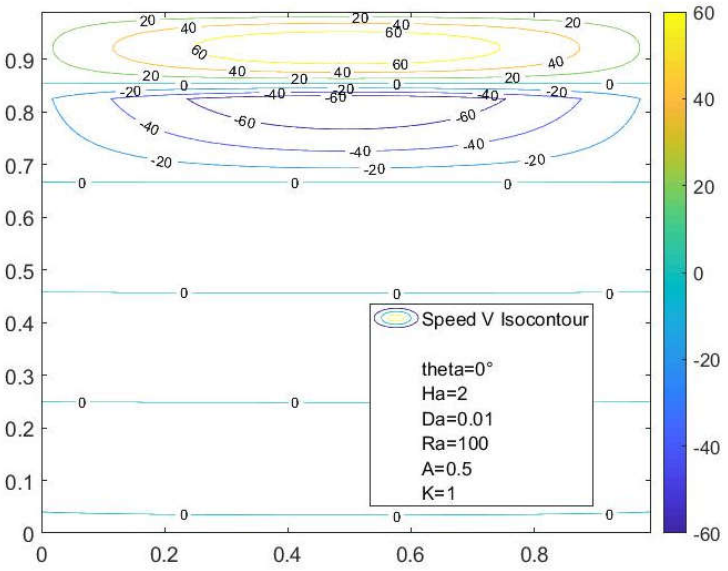

Figure 0-4: Speed V, Case Ha = 2

Case Ha = 3

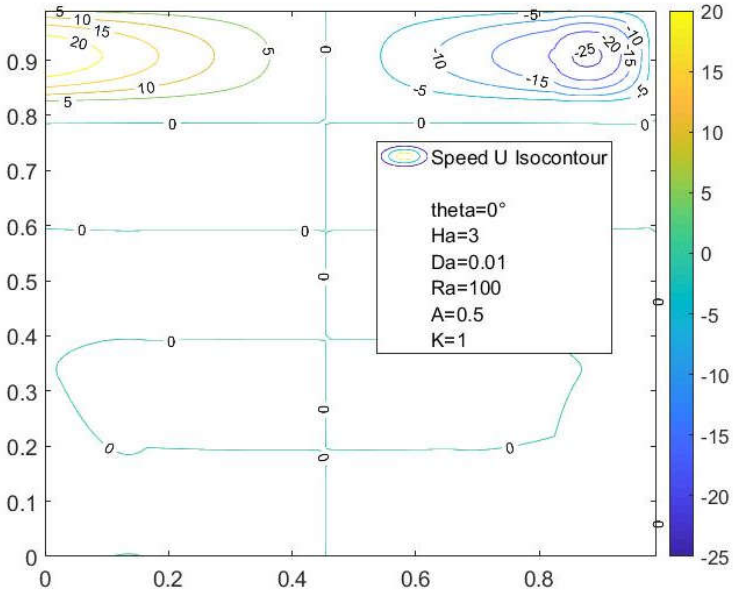

Figure 0-5: Speed U, Ha = Case 3

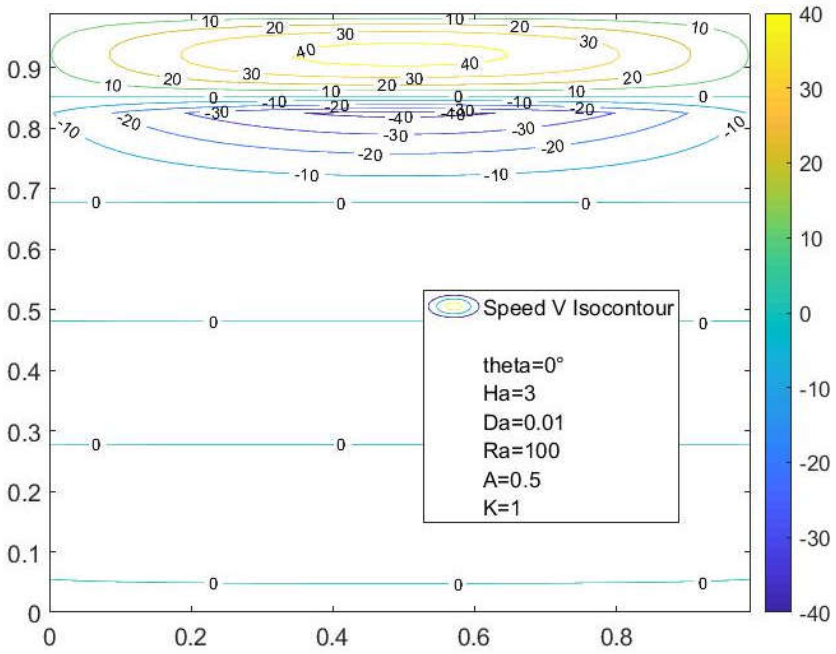

Figure 0-6: Speed V, Case Ha = 3

Case Ha = 4

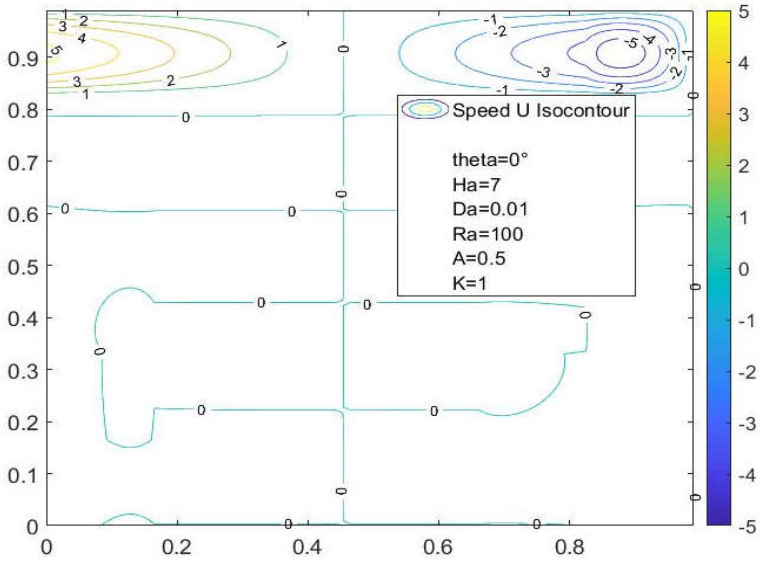

Figure 0-7: Speed U, Case Ha = 7

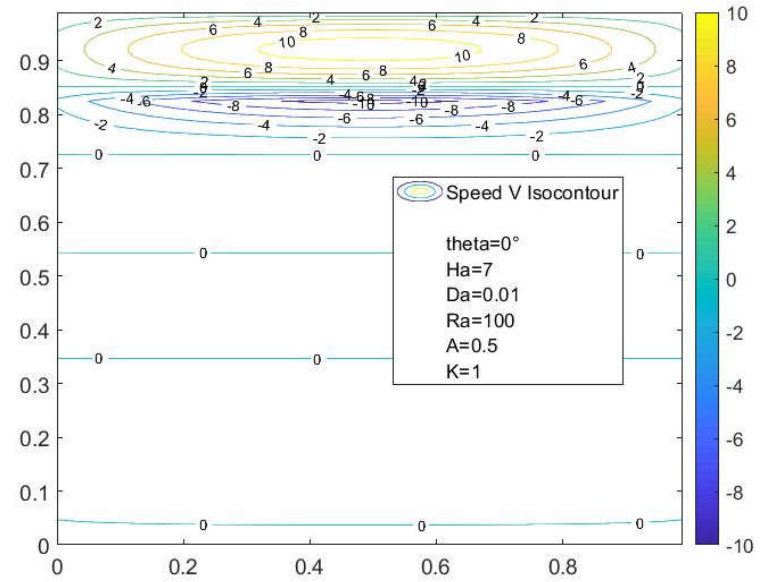

Figure 0-8: Speed V, Case Ha = 7

By observing the profiles obtained when Ha varies from 1 to 7, a progressive attenuation of the convective flow is noted. Indeed, the order of magnitude of the speeds is divided by 10 when Ha increases. Also, a symmetry of the flow field is observed concerning the central axis of the porous medium; which shows an inversion of the direction of flow each time the latter is in contact with the limiting horizontal walls of the enclosure. For different values of the Hartmann Ha number, it is noted that the velocity of the wall-flow is zero; which reflects the condition of adhesion to the wall relative to the generalized Brinkman model adopted.

Influence of Hartmann number Ha on the current lines

Case Ha = 1

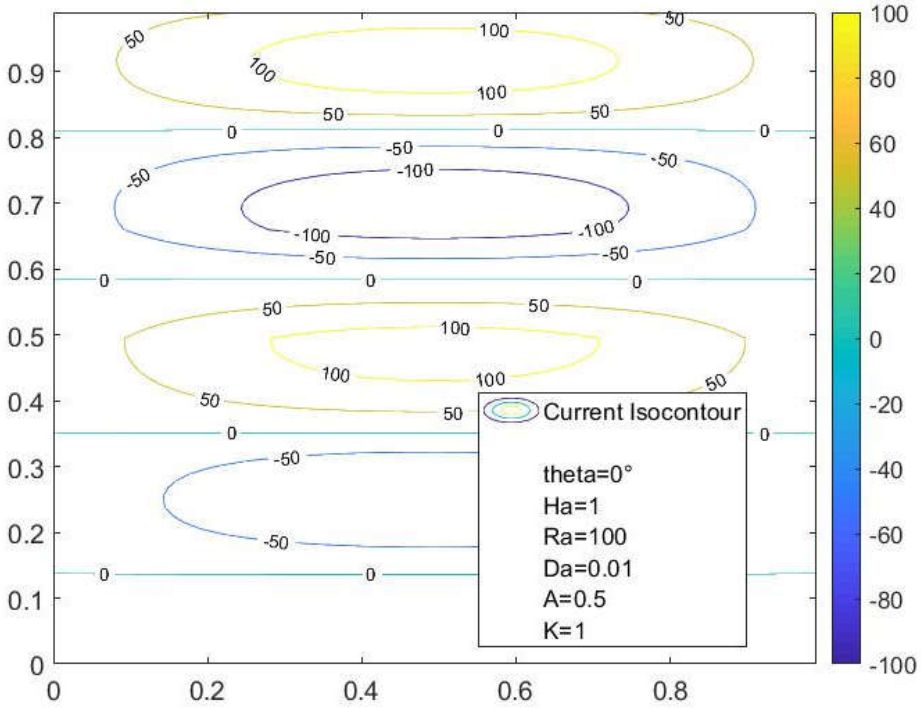

Figure 0-9: Streamlines, Case Ha = 1

Case Ha = 2

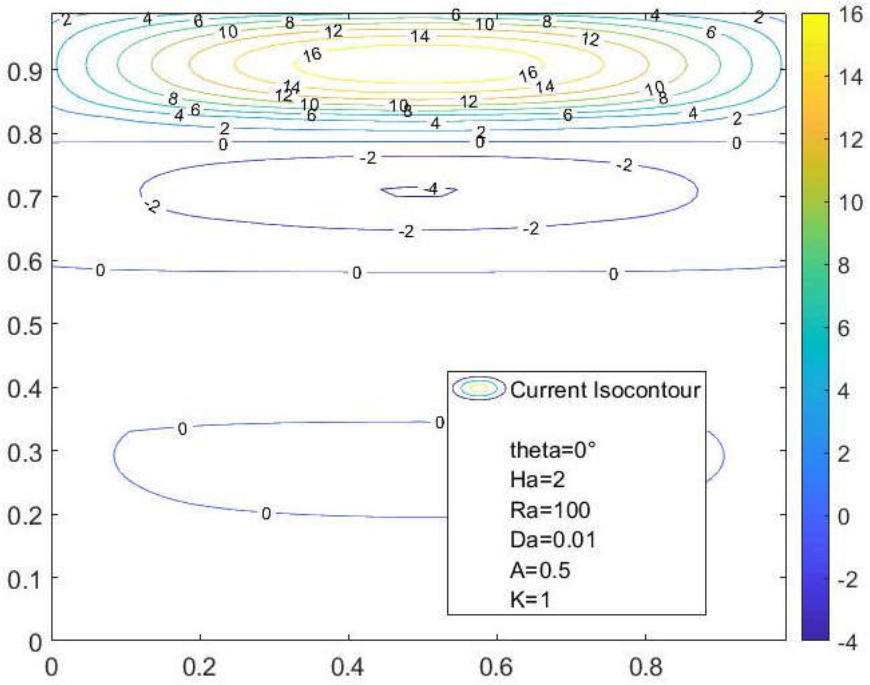

Figure 0-10: Streamlines, Case Ha = 2

Case Ha = 3

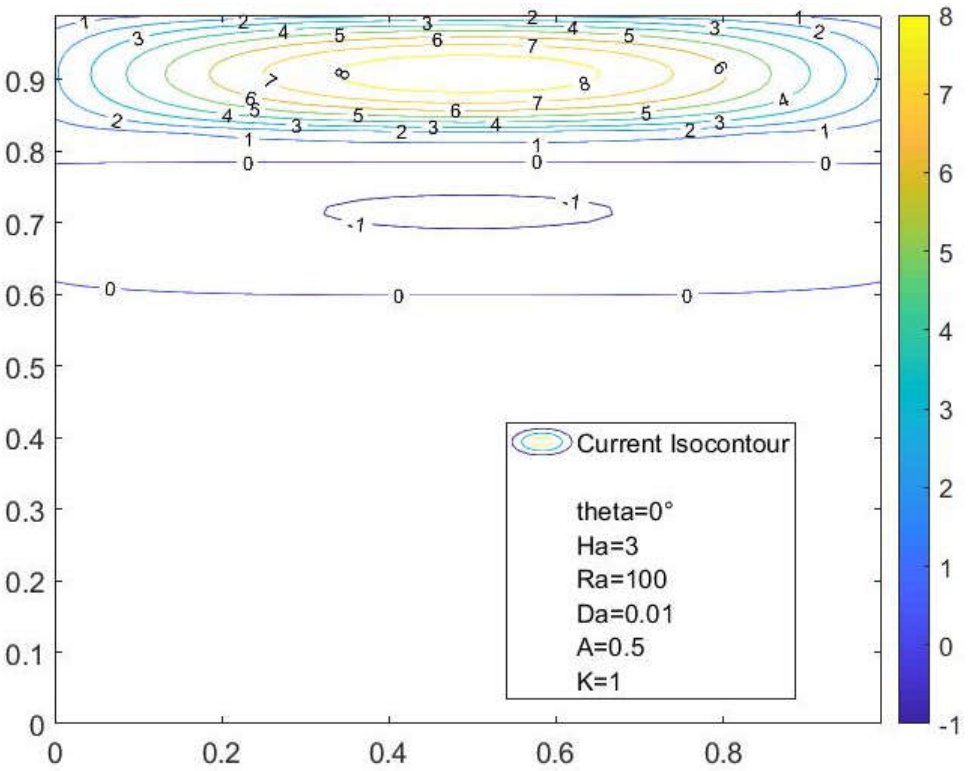

Figure 0-11: Streamlines, Case Ha = 3

Case Ha = 7

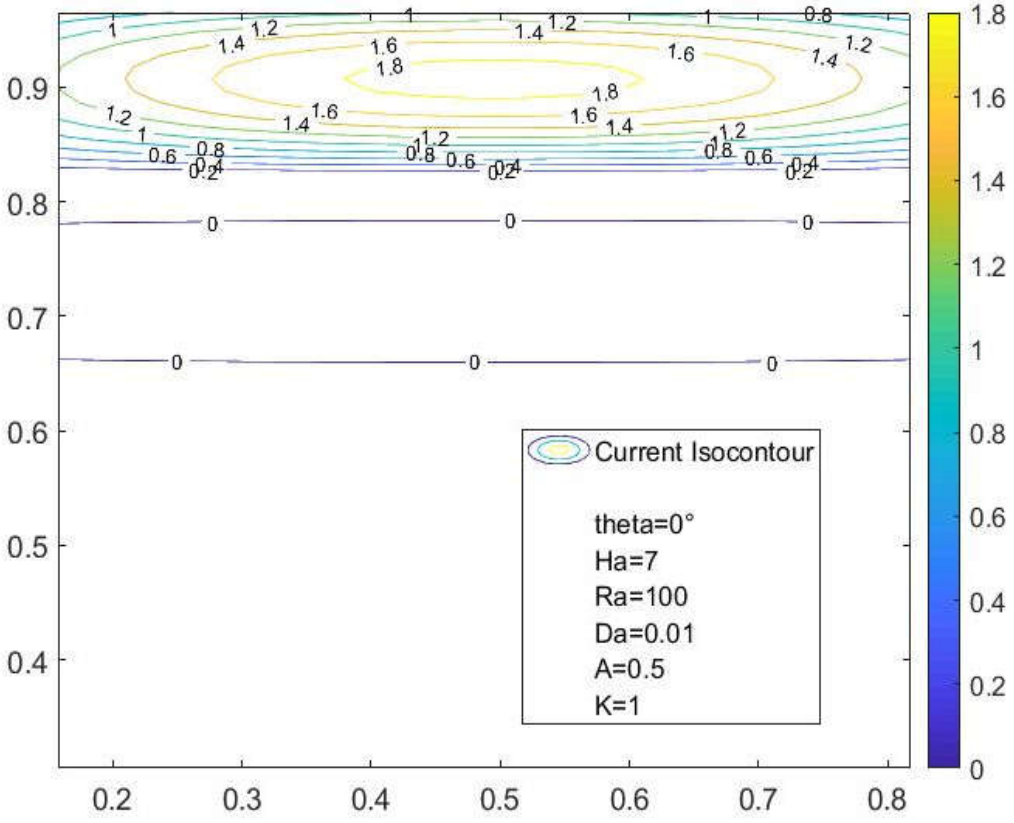

Figure 0-12: Streamlines, Case Ha = 7

The different profiles of current observed show the same trend as those of the speed *U* in terms of convective flow.

Influence of Hartmann number Ha on temperature lines

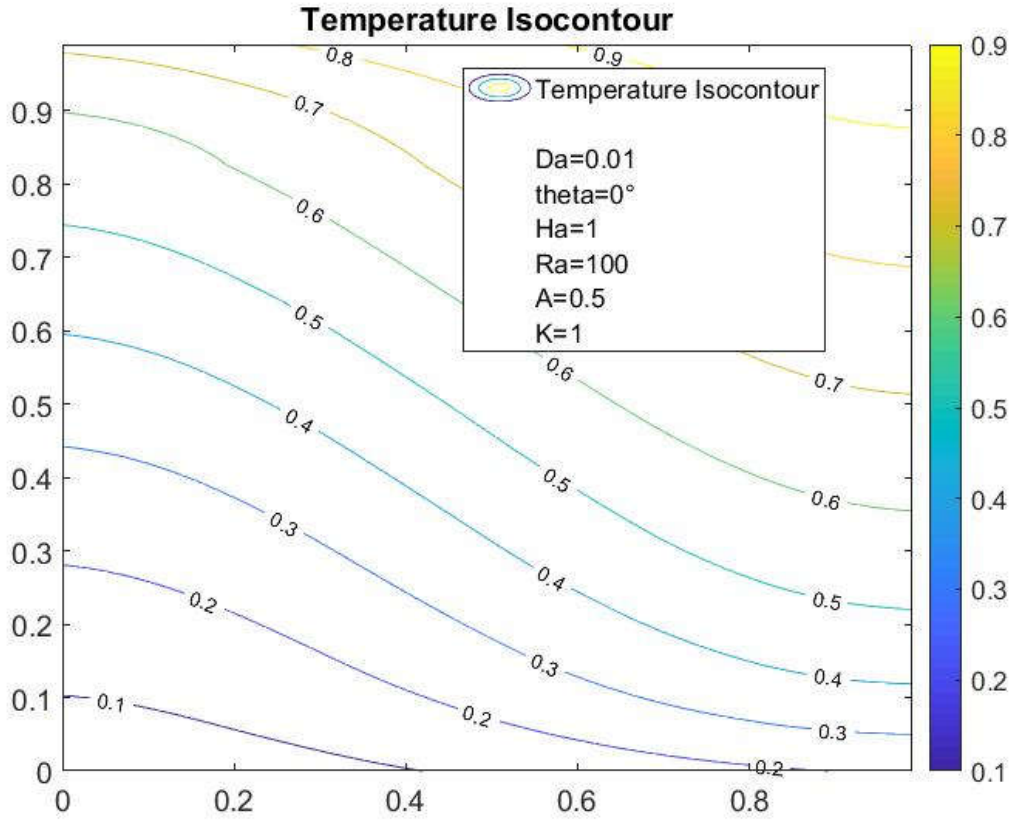

Figure 0-13: Temperature lines, Case Ha = 1

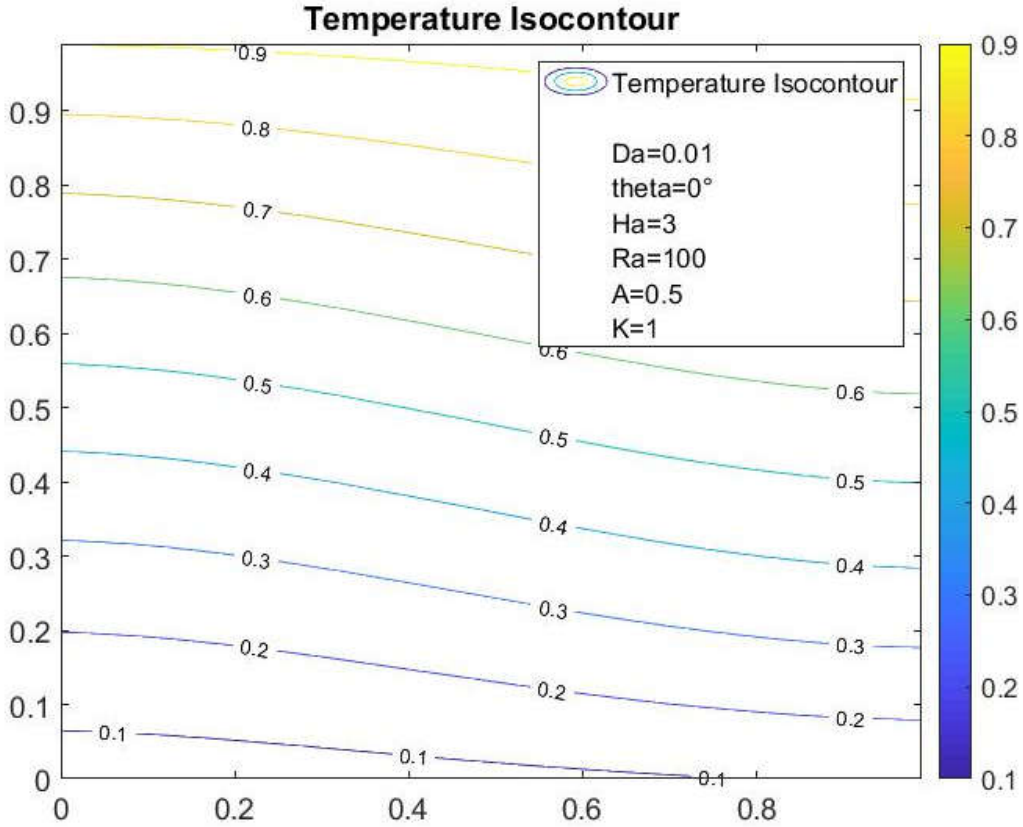

Figure 0-14: Temperature lines, Case Ha = 3

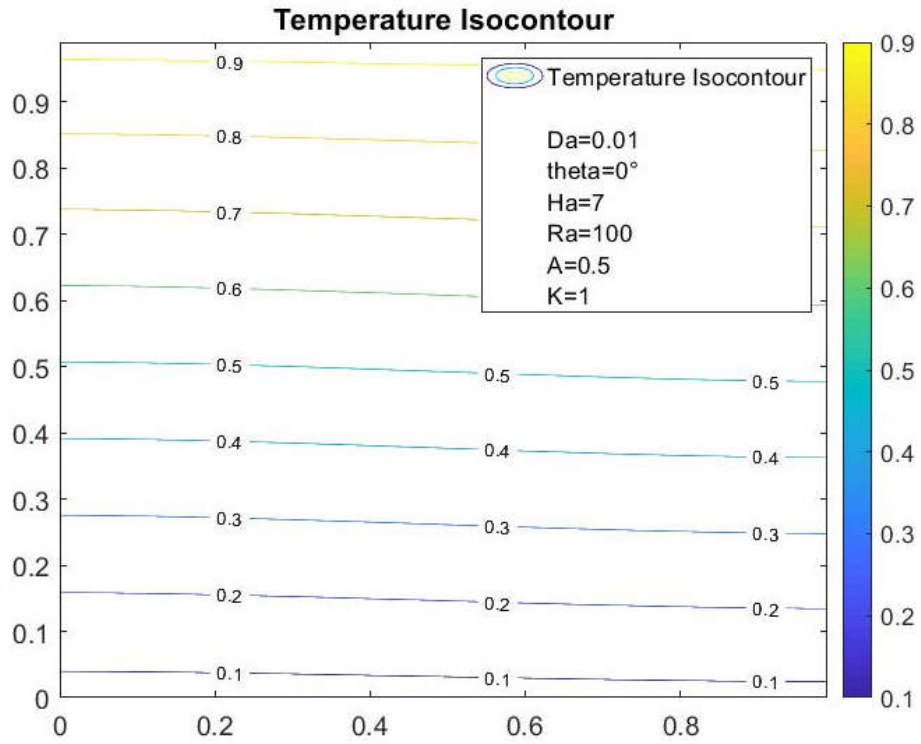

Figure 0-15: Temperature lines, Case Ha = 7

For $Ha \geq 7$: the isotherms are horizontal and almost parallel, it is therefore concluded that under these conditions the mode of transfer of heat by conduction is perfectly dominant (pure conduction).

For $Ha = 3$: isotherms show a slight deviation from the case of pure conduction

For $Ha \leq 1$: the isotherms show a significant deviation from the case of pure conduction. It is noted that the temperature distribution will be slightly variable according to the vertical axis, but variable according to the horizontal axis to satisfy the stable thermal stratification. It is concluded that under these conditions the mode of heat transfer by convection is dominant.

Heat transfer rate: Variations in the rate of heat transfer have been studied. according to several parameters, The results are presented through a few curves followed by their analyses.

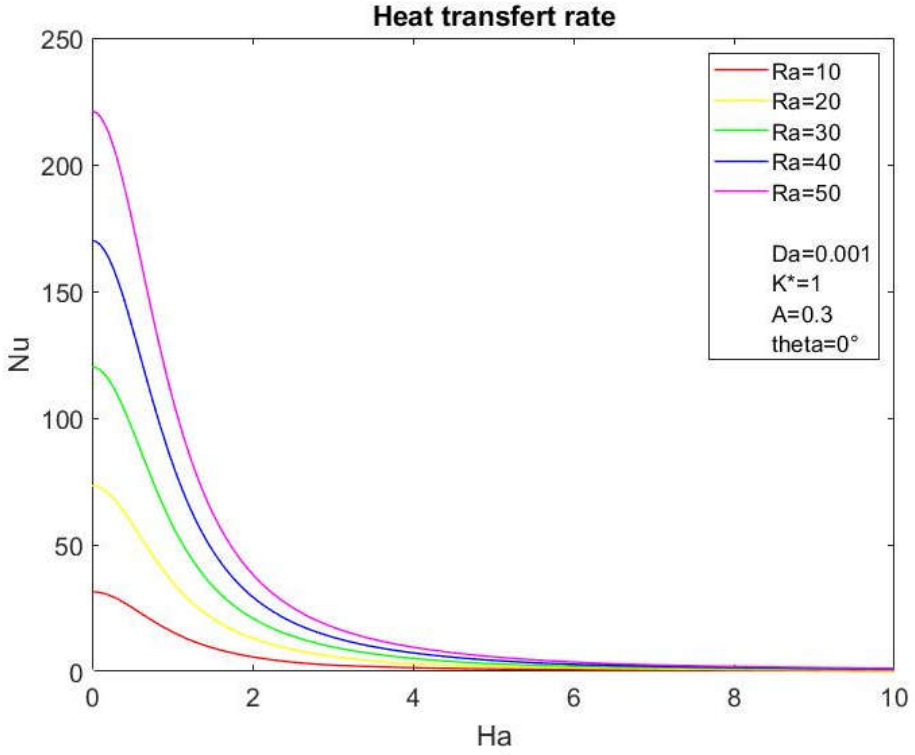

Figure 0-16: Ha effect on heat transfer for different Ra values

Figure 2-16 illustrates the variations in the heat transfer rate in porous media as a function of the Hartmann Ha number for different values of the Rayleigh *Ra* number when $Da = 0.001$, $K^* = 1$, $\theta = 0°$ and $A = 0.3$. This figure shows that the heat transfer by convection for each value of the Rayleigh *Ra* number decreases rapidly to reach the pure conduction regime for which $Nu = 1$ when the Hartmann *Ha* number increases. The *Ra* value for which the pure conduction regime is reached depends on the Hartmann number and thereby on the transverse magnetic field. Also, it is to be noted that the heat transfer by convection increases according to the value of the number of Rayleigh *Ra* when it is in the interval of low numbers of Hartmann *Ha (Ha <5).*

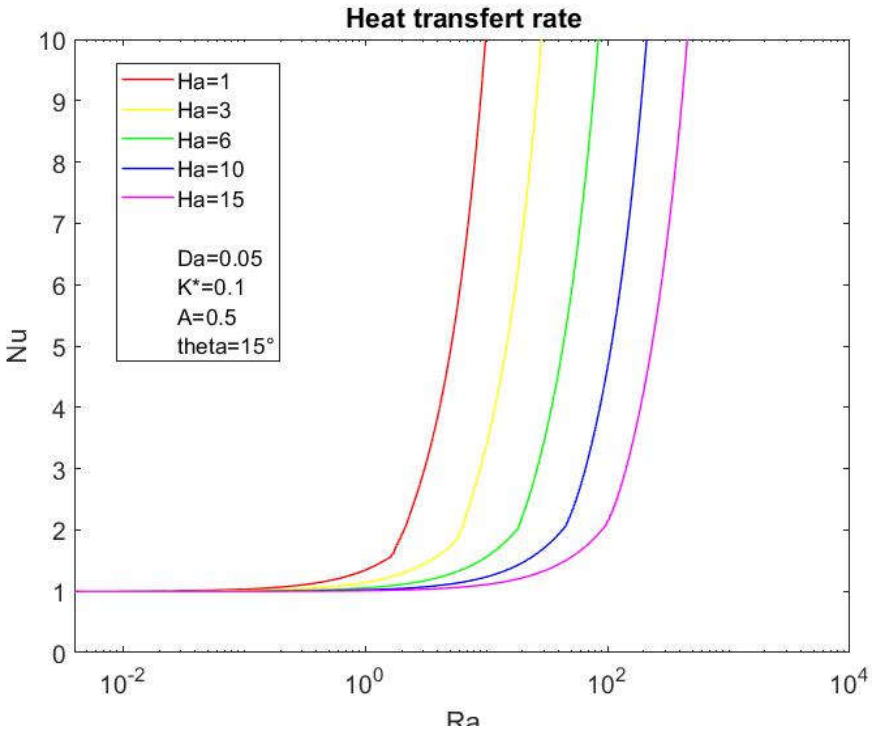

Figure 0-17: Ra effect on the heat transfer rates for different values of Ha

The effects of variation in the Hartmann *Ha* number on convective heat transfer as a function of the Rayleigh *Ra* number in the porous medium are shown in Figure 2-17. The analysis of the curves reveals that the rate of heat transfer by *Nu* convection increases from the pure conduction regime when *Ra* increases. Thus, for high Hartmann *Ha* values, heat transfer by convection is only possible within the limit of high Rayleigh *Ra* values. For a constant value of the Rayleigh *Ra* number, the increase of the Hartmann number significantly attenuates convective heat transfer.

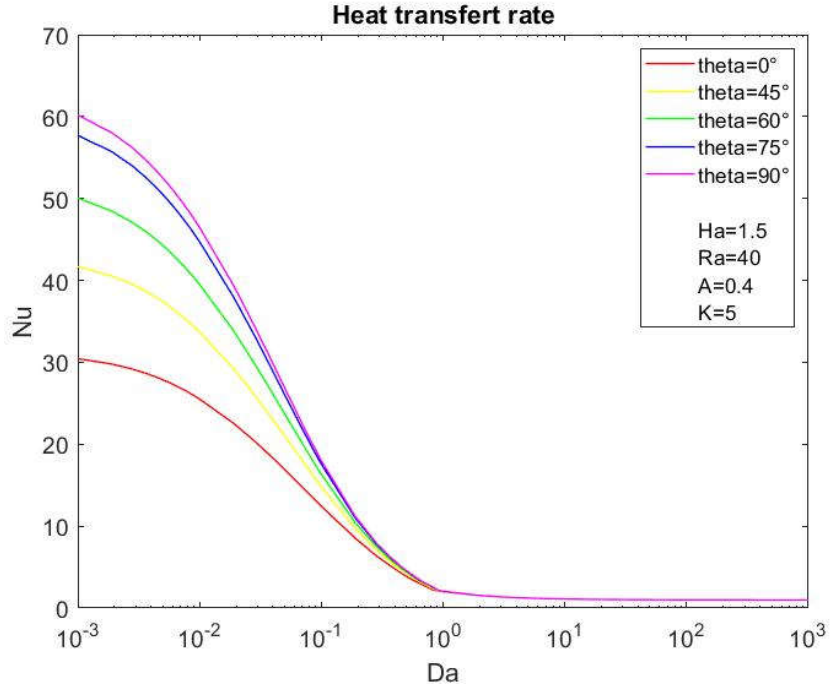

Figure 0-18: Da effect on the heat transfer rates for different values of θ

The value of the Darcy Da number to reach the pure conduction regime is independent of θ. For example for $Da \approx 10$, pure conduction is reached.

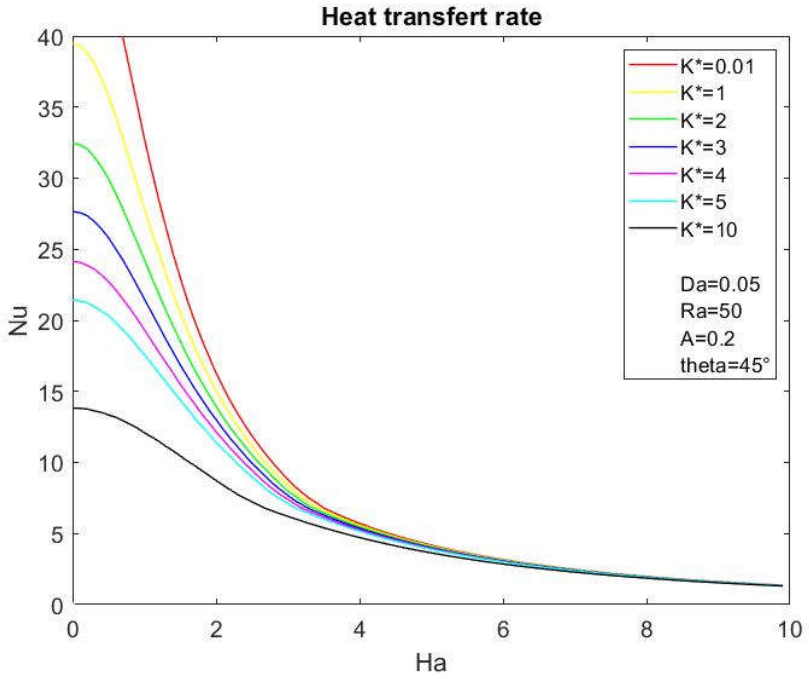

Figure 0-19: Ha effect on the heat transfer rate for various values of K*

From the analysis of the curves in Figure 2-19, it appears that the heat transfer by convection for each value of K^* decreases progressively until the pure conduction regime is reached for which $Nu = 1$ when Ha increases. The value of K^* for which the pure conduction regime is reached depends on the Hartmann number, therefore on the transverse magnetic field. For example for $K^* = 4$ when $Ha = 2.5$, the pure conduction regime is almost reached. It should also be noted that the heat transfer by convection increases with the increase in the Hartmann number when the anisotropy ratio in K^* permeability of the porous medium decreases. Therefore, it follows from this analysis that, when $\theta = 45$ °, the heat transfer increases when the permeability of the porous medium in the horizontal direction is higher compared to that prevailing in the vertical direction ($K^* < 1$) and decreases when the opposite situation is witnessed for which $K^* > 1$.

Conclusion

This study relates to natural magnetohydrodynamic convection in a rectangular cavity isothermally heated by the sides and filled with an anisotropic porous material. This cavity is subjected to the action of a transverse magnetic field. From the data collected and analyzed, the following conclusions emerge:

- the convective flow is greatly influenced by the anisotropy parameters of permeability for the porous layer and by the effect of the transverse magnetic field applied.
- the rate of heat transfer in the porous medium increases when the permeability in the horizontal direction is higher than that prevailing in the vertical direction
- the increase in the intensity of the transverse magnetic field applied reduces significantly the velocity of the flow of the fluid saturating the porous medium and thereby attenuates the transfer of heat by convection in the medium.

REFERENCES

(1) SEBASTIEN RENAUDIERE DE VAUX, 2017, Convection thermique en présence d'un champ magnétique constant, alternatif,ou d'une source de chaleur dispersée.<https://oatao.univ-toulouse.fr/19752/1/renaudiere.pdf>
(2) BENNACER, R., TOBBAL, A., BEJI, H.,2002,Convection naturelle thermosolutale dans une cavité poreuse anisotrope : Formulation de Darcy-Brinkman.http://www.cder.dz/download/Art5-1_1.pdf
(3) VENKATACHALAPPA M. and SUBBARAYA C. K., 1993, Natural Convection in a Rectangular Enclosure in the Presence of a Magnetic Field With Uniform Heat Flux From the Side Walls<https://page-one.springer.com/pdf/preview/10.1007/BF01340696>
(4) MAHIDJIBA, A., 2001, Convection naturelle en milieu poreux anisotrope-Effet du maximum de densité, thesis, University of Montéal, pp. 152. <http://www.collectionscanada.gc.ca/obj/s4/f2/dsk3/ftp05/NQ65544.pdf>

(5) AKOWANOU Chr., DEGAN, G., 2007,Transfert convectif dans les cavités poreuses soumises à un champ magnétique transversal. J. Rech. Sci. Univ. Lomé (Togo), série E, 9(1): 1-11.<http://bec.uac.bj/uploads /publication/ 0e8fl6a0fc8ea 88c2986310288409866.pdf>

(6) André Fortin, 2016, Analyse numérique pour ingénieurs, ISBN13 : 978-2-553-01680-6, collection : Cursus, Editeur :**Ecole** Polytechnique de Montréal**,** pp. 480.

(7) Jean-Louis Merrien, 2007, ANALYSE NUMÉRIQUE AVEC MATLAB, Collection : Sciences Sup, Dunod, pp. 216.

(8) Christophe ROLAND, 2005, Méthodes d'Accélération de Convergence en Analyse Numérique et en Statistique, thesis, Université des Sciences et Technologies de Lille U.F.R. de Mathématiques Pures et Appliquées, pp. 146.

(9) GOURI DHATT; GILBERT TOUZOT, 1981,Une présentation de la méthode des éléments finis,Collection Université de Compiègne, ISSN 0180-2976, Publisher : Maloine, ISBN : 2224007000, 9782224007003, pp. 543.

(10) Vincent Manet, 2013, La Méthode des Éléments Finis: Vulgarisation des aspects mathématiques, Illustration des capacités de la méthode. DEA. Eléments finis pour l'ingénieur, ViM2, Lyon, pp. 355.cel-00763690v3

(11) BELAHMADI E., 2013, Simulation numérique de la convection naturelle dans une cavité carrée poreuse, Master, Mechanical engineering, University of Constantine 1, pp. 103. http://bu.umc.edu.dz/theses/gmecanique/BEL6418.pdf